JOURNAL OF Materials CHEMISTRY

Titania–silica doped with transition metals *via* flame synthesis: structural properties and catalytic behavior in epoxidation

Wendelin J. Stark,[a,b] Reto Strobel,[a,b] Detlef Günther,[c] Sotiris E. Pratsinis[b] and Alfons Baiker[a]

[a]*Laboratory of Technical Chemistry, ETH Hönggerberg, CH-8093 Zurich, Switzerland. E-mail: baiker@tech.chem.ethz.ch*
[b]*Institute of Process Engineering, ETH Zentrum, CH-8092 Zurich, Switzerland*
[c]*Laboratory of Analytical Chemistry, ETH Hönggerberg, CH-8093 Zurich, Switzerland*

Received 8th August 2002, Accepted 9th October 2002
First published as an Advance Article on the web 15th October 2002

The influence of trace amounts of transition metals (Cr, Mn, Fe, Co) on the structural and catalytic properties of silica and 1 wt% titania–silica nanoparticles prepared by flame synthesis has been investigated. The transition metal concentration was varied from 40 to about 2000 ppm by admixing the corresponding transition metal precursor to the silica and titania–silica precursor mixtures. These components were fed into a methane–oxygen diffusion flame, affording a single-step flame synthesis of the mixed oxide materials. The specific surface areas of all the powders thus prepared ranged from 60 to 240 $m^2\ g^{-1}$, with oxygen flow being the most influential parameter. Diffuse reflectance UV-VIS and FT-IR spectroscopy showed that the Ti sites in the doped nanoparticles were unaffected by chromium, manganese, and cobalt, while iron led to the formation of a dual site with considerable acidity. Epoxidation of 2-cyclohexenol by *tert*-butylhydroperoxide (TBHP) was used to probe the effect of the transition metal dopants on the activity and selectivity of the titania–silica. A significant loss in selectivity to the epoxide was observed for all doped mixed oxides. The chromium-doped material was highly active, favoring radical processes. Even at a doping level of 40 ppm, considerable amounts of ketone by-products were formed. Manganese doping led to slow decomposition of the TBHP, but had no significant influence on the alkene conversion at Mn contents of up to 2000 ppm. Incorporation of iron afforded Lewis acid sites, leading to dehydration activity, as demonstrated by the occurence of water abstraction from the reactant. Cobalt-doped titania–silica showed only a weak tendency toward radical reactions, and no reactions due to Lewis acid sites were observed. Among the metal dopants, only chromium underwent significant leaching under reaction conditions.

1 Introduction

Titania–silica is one of the most active mixed oxide catalysts for liquid-phase oxidations. It is particularly active in the epoxidation of alkenes and allyl alcohols by hydroperoxides and has become an important industrial catalyst for the production of propylene oxide.[1] Ever-increasing demands for clean oxidation processes with high product selectivity to avoid by-product and waste formation has led to considerable research efforts in this area. Numerous publications deal with transition metals on carrier oxides and most 3d metals show some oxidation activity. However, product selectivity in general is often low and homogeneous reactions always compete with reactions on the catalyst surface. Many transition metals are prone to leaching, which leads to product contamination with heavy metals and fast catalyst deactivation.[2] The liquid-phase oxidation of alkenes with titania–silica is particularly sensitive to contamination.[1] The level of impurity has been shown to be one of the most decisive properties determining the catalytic behavior of these materials.[3,4] Wet-phase catalyst preparation entrains metal contamination from production equipment.[5] In contrast to this, flame aerosol processes can easily produce highly pure materials, as has been demonstrated, for example, in the manufacture of optical fibers.[6,7]

This prompted us to systematically study the influence of trace amounts of chromium, manganese, iron, and cobalt on the structural and catalytic properties for liquid-phase epoxidation of titania–silica prepared *via* flame synthesis. Epoxidation of 2-cyclohexenol by *tert*-butylhydroperoxide (TBHP) was used as a test reaction.[8] Co-operative effects and the formation of dual sites involving two transition metals have been investigated using reference silica powders with the same metal contents, but no titania.

2 Experimental

2.1 Materials preparation and characterization

Titania–silica powders containing low concentrations of different transition metals were prepared by feeding the corresponding volatile precursors into a methane–oxygen co-flow diffusion flame.[9] The reactor consists of three concentric stainless-steel tubes with inner diameters of 2.5, 4.0, and 5.5 mm, and a wall thickness of 0.3 mm. An argon stream flowing at 1 L min^{-1} carrying the precursor vapors was introduced through the center tube, methane flowed through the inner annulus at a rate of 0.5 L min^{-1}, while 2–10 L min^{-1} of oxygen flowed through the outer annulus, resulting in a simple diffusion flame.[10] All gases (Pan Gas, purity > 99.999%) were delivered from cylinders with the flow rates being monitored by calibrated mass flow controllers (Bronkhorst EL-Flow F201). Mixtures of titanium tetraisopropoxide (TTIP; Aldrich, >97%; distilled under vacuum prior to use) and hexamethyldisiloxane (Fluka, purum, >99%; distilled over liquid sodium prior to use) were prepared and stored separately. The mixture was fed into an evaporator (Bronkhorst CEM 100W) at a flow rate of 10 g h^{-1} controlled by a liquid mass flow meter (Bronkhorst Liqui-Flow L1) and evaporated into an argon stream flowing at 0.5 L min^{-1}. A second evaporator was used

 DOI: 10.1039/b207782e

Table 1 Precursors used for the introduction of different transition metals in silica and titania–silica

Name and chemical formula	Boiling point/K	Properties
Titanium tetraisopropoxide, $Ti(OC_3H_7)_4$	513	Moisture sensitive
Chromium hexacarbonyl, $Cr(CO)_6$	430 (dec.)	Toxic
Dimanganese decacarbonyl, $Mn_2(CO)_{10}$	427 (dec.)	Air sensitive, toxic
Ferrocene, $Fe(C_5H_5)_2$	522	
Cyclopentadienylcobalt dicarbonyl, $Co(C_5H_5)(CO)_2$	413	Air sensitive, toxic

to vaporize a solution of the dopant precursor in toluene (Fluka, >99.5%; dried over molecular sieves 4A) at a flow rate of 7.5 g h^{-1} into an argon stream flowing at 0.5 L min^{-1}. Table 1 lists the different precursors used in this study.

All mixtures and precursors were handled with the exclusion of air and moisture using standard Schlenck techniques. Since less than 0.2 wt% dopant was added, the composition of the gases changed very little and the fuel content in the flame was almost constant throughout all experiments.[11] Both evaporators, the precursor delivery tubes, and the burner were heated to 160 °C to prevent condensation of precursor vapor. The flame was surrounded by a quartz chimney (glass cylinder, i.d. = 140 mm) to maintain stable combustion. A stainless steel filterholder with a glassfiber filter (Whatman GF/A) was mounted on top of the cylinder. Product particles were collected on the filter with the aid of a vacuum pump (Vacuubrand RE 5). Each experiment was reproduced at least twice. The different materials are designated *x*TS, where *x* represents the amount of the transition metal (TS) in the silica in ppm, and *x*TSTi (titania–silica) containing *x* ppm transition metal.

Specific surface area and isotherms. The specific surface areas of the collected powders were analyzed by nitrogen adsorption at 77 K using the BET method (Micrometrics GEMINI 2360). The results were cross-checked by recording a full adsorption isotherm (Micrometrics ASAP 2010 Multigas system).

Laser ablation ion-coupled plasma mass spectrometry. Samples were pressed into plates and irradiated with an excimer laser (Lambda Physik Compex 110 I; ArF, 193 nm, pulse energy 150 mJ, frequency 10 Hz) with a spot diameter of 40 μm. The vaporized sample was carried by a helium stream to a quadrupole ICP mass spectrometer (Perkin Elmer Elan 6100) and analyzed for all 3d metals and silicon. Details of the instrumentation are given in ref. 12 and 13. Calibration was carried out with NIST 610 glass standards. The nominal and measured chemical compositions are listed in Table 2.

Diffuse reflectance UV-VIS spectroscopy. DRUV-VIS spectra were recorded on a Varian Cary 500 instrument equipped with a Praying Mantis diffuse reflectance unit and a Harrick reaction chamber with heat controller and a gas flow system. Samples were measured against a barium sulfate background at 60 nm min^{-1} and a step size of 1 nm. The powders were analysed at 50 (hydrated) and 300 °C under flowing argon (dehydrated).

Diffuse reflectance FT-IR spectroscopy. DRIFT spectra were recorded on a Bruker Vector 22 instrument equipped with a Praying Mantis diffuse reflectance unit and a Harrick reaction chamber with heat controller and a gas flow system. Samples were diluted tenfold in KBr and 512 scans measured against a KBr background at a resolution of 4 cm^{-1} from 4000 to 500 cm^{-1}.

2.2 Catalytic activity

The epoxidations were carried out batchwise in a mechanically stirred, 50 ml thermostatted glass reactor equipped with a thermometer, reflux condenser, and a septum for withdrawing samples.[14] All reactions were performed under nitrogen (99.999%) to exclude oxygen and moisture. In a standard procedure, 100 mg of mixed oxide was predried *in situ* in the reactor under flowing nitrogen for 15 min at 423 K. After cooling, 8.05 ml of toluene (Fluka, 99.8%; stored over molecular sieves 4A) as solvent and 0.5 ml dodecane (Fluka, 99%) as an internal standard were added. The mixture was heated to 363 K and 1 ml of 2-cyclohexenol (Fluka, 99%) was injected. The reaction was started by introducing 0.45 ml *tert*-butylhydroperoxide (TBHP; 5.4 M in decane, Fluka; stored over molecular sieves 4A). The total reaction volume was 10 ml. For leaching experiments, 2 ml of the reaction mixture were filtered hot through a dry, preheated membrane filter (pore diameter 0.2 μm).[2,15] The filtrate without catalyst was kept at 90 °C and the concentrations of all species were monitored as for normal runs. Tests for metal leaching were carried out for reaction mixtures at 50% peroxide conversion. The mixtures were analyzed using a Trace 2000 gas chromatograph equipped with a cool on-column inlet and an HP-FFAP capillary column. Products were identified by GC-MS and by comparison with authentic samples. In all runs, the internal standard method was used to quantitatively analyze all components. The epoxide selectivity, related to the alkene consumed, S_{Chxol}, and the peroxide selectivity, S_{perox}, related to the consumed TBHP were calculated from,

$$S_{Chxol}\ (\%) = 100\{[epoxide]/([Chxol]_0 - [Chxol])\}$$

$$S_{perox}\ (\%) = 100\{[epoxide]/([TBHP]_0 - [TBHP])\}$$

where the subscript 0 indicates an initial value and all concentrations are expressed on a molar basis. The rates of epoxide formation was compared after 1 h and the product selectivity calculated at 50% conversion.

Table 2 Nominal and measured chemical composition of catalytic materials

Sample	Ti content/wt%	Dopant content	Sample	Ti content/wt%	Dopant content
Si	0.0001[a]	3 ppm Fe	Ti	1.3	3 ppm Fe
40Cr[b]	1.1	60 ppm Cr	100Fe	1.4	130 ppm Fe
400Cr	1.1	440 ppm Cr	1000Fe	1.2	780 ppm Fe
2000Cr	0.9	1970 ppm Cr	2000Fe	1.2	2280 ppm Fe
50Mn	1.3	60 ppm Mn	40Co	1.2	30 ppm Co
500Mn	1.3	480 ppm Mn	400Co	1.2	640 ppm Co
2000Mn	1.0	1930 ppm Mn	2000Co	1.1	1680 ppm Co

[a]Limit of detection. [b]Numbers indicate the nominal dopant content in weight% of the corresponding oxide M_2O_3 (M = Cr, Mn, Fe, Co).

3 Results and discussion

3.1 Powder production

Fig. 1 shows the BET specific surface areas of silica containing 0.2 wt% of different transition metal dopants as a function of the employed oxygen flow rate in the flame. The inset depicts a typical flame producing manganese-doped silica nanoparticles (10–20 nm). At low oxygen delivery, long hot flames favor particle sintering, leading to larger particles with low specific surface areas.[10] Increasing the oxygen flow rate shortens the flame by enhanced reactant mixing and faster reaction, thus reducing the high temperature particle residence time. Particles have less time for sintering and growth and the specific surface area of the non-porous materials can reach up to *ca.* 250 m^2 g^{-1}.[8] The influence of different transition metals is best observed with powders of high specific surface area (*i.e.* prepared using an O_2 flow rate of 8–10 L min^{-1}). The addition of 0.2 wt% chromium or iron oxide reduced the specific surface area by about 20%, while cobalt and manganese showed less of an influence. Since high specific surface area is generally favorable in titania–silica catalysts, a series of samples with increasing dopant concentrations was prepared in flames with a constant O_2 flow rate of 8 L min^{-1}. To trace the influence of transition metals on the epoxidations, both samples with about 1 wt% titania and reference samples based on pure silica were prepared. The dopant concentration was varied from 40 to 2000 ppm nominal transition metal oxide (weight of oxide) by mixing appropriate amounts of the metal precursor into the silica and titania–silica precursor mixtures.

Table 2 lists the dopant contents of the samples as determined by Laser ablation ICP-MS. The composition could be controlled quite well; some of the deviations can be attributed to the difficulty of mixing small amounts of liquids under Schlenck conditions. This confirms that, in most cases, the precursors can be evaporated and transported to the flame without significant decomposition or wastage, thus preserving the mass balance in the flame reactor setup. Table 2 further lists the titania contents of all the samples, some deviation from the nominal value was found due to the high sensitivity of the precursor TTIP to moisture and prolonged storage in dilute solution. However, it has been demonstrated previously that, within this range of Ti content, no significant change in epoxidation selectivity occurs.[8] The specific surface areas of all the powders are between 190 and 240 m^2 g^{-1}, which allows direct comparison of activity.

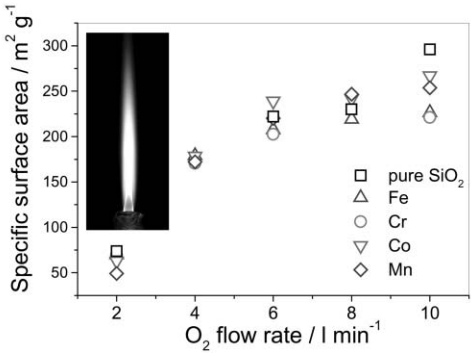

Fig. 1 Specific surface areas of silica nanoparticles doped with 0.2 wt% of transition metal oxides. The surface area increases significantly as the oxygen flow rate is raised since enhanced mixing drives the reaction and entrainment of ambient air affords faster cooling and smaller particles. The addition of transition metals increases the sintering properties of silica and larger particles with lower specific surface areas are formed. The inset shows a typical methane–oxygen diffusion flame producing Mn-doped silica nanoparticles.

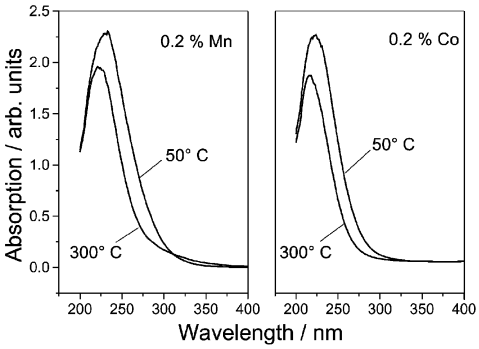

Fig. 2 *In situ* DRUV-VIS spectra of as-prepared (50 °C) and dehydrated Mn- and Co-doped titania–silica. The broad peak of slightly hydrated, single Ti sites in silica narrows considerably at 300 °C under flowing argon, indicating the loss of water. This confirms that both Mn and Co have no influence on the Ti site distribution in the silica.

3.2 Materials characterization

Fig. 2 compares the DRUV-VIS spectra of Mn- and Co-doped titania–silica as prepared (hydrated, 50 °C) and after dehydration (300 °C). The hydrated spectra show a broad peak at 220 nm. Upon heating, this peak narrows significantly. No apparent differences emerge for the two different metals. The Ti species in flame synthesis titania–silica have been shown by *in situ* XANES to be mostly tetrahedral.[16] This agrees with the appearance of a narrow peak at 220 nm.[17] The removal of weakly bound hydration water results in the characteristic narrowing of the peak upon heating.[18]

Fig. 3 shows DRUV-VIS spectra of Cr-doped silica, and Cr-doped titania–silica for different temperatures. The spectra of Cr-doped silica exhibit a peak at around 240 nm that is unaffected by heating under flowing argon, whereas the peak at 340 nm disappears gradually upon heating under flowing argon. The spectrum of Cr-doped titania–silica is a combination of the individual spectra of the two metals. Heating the sample under flowing argon leads to the same reduction of the peak at 340 nm as observed for Cr-doped silica, while the signal at 240 nm remains in the spectrum in the form of a shoulder. It may be concluded that the two metals do not form a dual site and that the addition of Cr has no measurable influence on the Ti sites.

Fig. 4 shows the DRUV-VIS spectrum of Fe-doped silica, titania–silica, and Fe-doped titania–silica. Note that the spectrum of Fe-doped silica has been magnified 50 times; it is characterized by the appearance of a peak at 255 nm, which is assigned to single Fe(III) ions.[19] This charge transfer band has

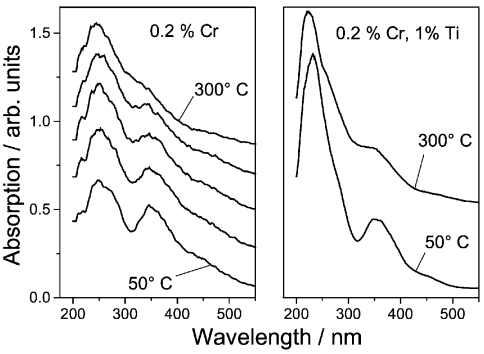

Fig. 3 *In situ* DRUV-VIS spectra of 0.2 wt% $CrO_{1.5}$–silica (left) at increasing temperatures under flowing argon. The peak at 340 nm shrinks considerably, while the signal at 240 nm remains unaffected. The same behavior is found for Cr-doped titania–silica (right). Its spectrum is a combination of the spectra of Cr-doped silica and Ti-doped silica. Addition of Cr has no significant influence on Ti site formation.

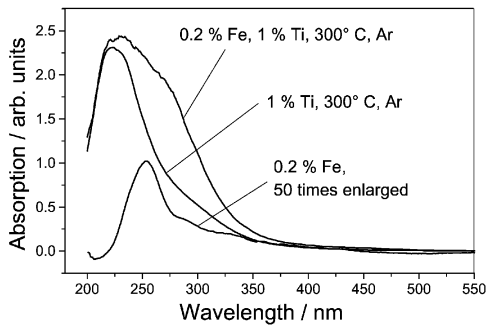

Fig. 4 *In situ* DRUV-VIS spectra of Fe-doped silica (magnified 50 ×), titania–silica, and Fe-doped titania–silica. The addition of Fe to titania–silica leads to considerable peak broadening. This cannot be explained by the presence of Fe only, since the reference spectrum of Fe-doped silica shows a weak signal. The catalytic activity of the ternary oxide Fe-doped titania–silica is also not just a superposition of the individual activities of Fe-doped silica and titania–silica. These results suggest the formation of a dual site containing both Fe and Ti.

previously been observed in other Fe-doped silica samples.[20–22] The absence of peaks at higher wavelengths indicates high Fe dispersion and a narrow species distribution. While the spectrum of titania–silica shows the characteristic narrow peak at around 220 nm for isolated Ti sites in silica, the addition of 0.2 wt% $FeO_{1.5}$ leads to considerable peak broadening. The spectrum of Fe-doped titania–silica cannot be a combination of the spectra of titania–silica and Fe-doped silica since the intensity of the spectrum of the latter is too weak to cause the broad signal observed in the spectrum of the former. Ma *et al.* prepared an iron- and titanium-containing zeolite and proposed the formation of a dual site in Ti-Fe-ZSM-5.[23] The formation of a similar dual site in Fe-doped silica–titania, containing both Fe and Ti in close proximity, may explain the observations made from the spectra in Fig. 4, which agree with the catalytic results.

Fig. 5 compares the DRIFT spectra of silica, 0.2 wt% $FeO_{1.5}$–silica, 1.2 wt% TiO_2–silica, and 0.2 wt% $FeO_{1.5}$–1.2 wt% TiO_2–silica at 50 °C and at 300 °C under flowing argon. In all spectra, the band at 800 cm^{-1}, assigned to symmetric Si–O–Si stretching vibrations, is taken as a reference to compare the spectra.[24] This is justified by the fact that the silica content is constant within 99% in all samples. Pure silica shows a small shoulder at around 980 cm^{-1} that results from Si–OH groups.[25,26] Most of these are removed upon heating, resulting in the loss of the corresponding shoulder (A). Adding iron to the silica results in a weak shoulder at 950 cm^{-1} in the cold spectrum. Maxim *et al.* recently prepared Fe-doped silica by pyrolysis of an organic precursor and attributed this shift to the presence of Fe–O–Si bonds.[27] No bands characteristic of iron oxide or hydroxides are observed. The shifted Si–OH shoulder disappears after heating, confirming that Fe–O–Si species are not detectable at this low concentration. The spectrum of titania–silica shows a band at 960 cm^{-1} that is attributed to Ti–O–Si species and Si–OH groups.[28] Upon dehydration, the intensity of this band is strongly reduced. The Ti–O–Si band is weak compared to the Si–OH band. In the case of the spectrum of ternary Fe-doped titania–silica, the peak at 960 cm^{-1} is more intense than for pure titania–silica. Again, the signal is reduced to a small shoulder on heating to 300 °C. This indicates that the ternary oxide forms more Si–OH than pure titania–silica.

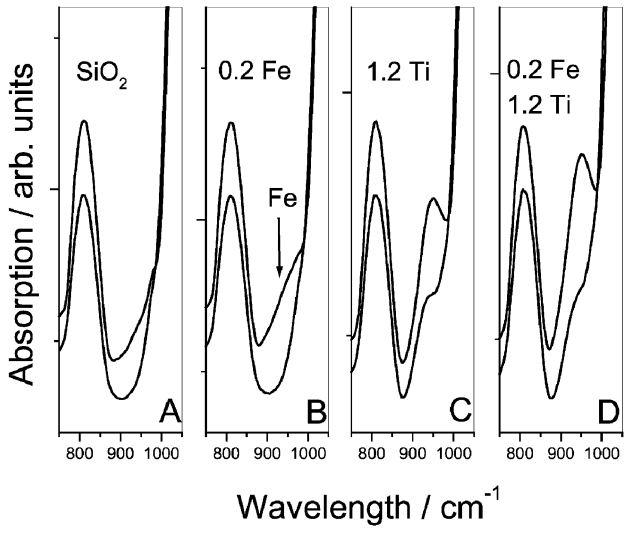

Fig. 5 *In situ* DRIFT spectra of silica (A), 0.2 wt% $FeO_{1.5}$–silica (B), 1.2 wt% TiO_2–silica, (C), and 0.2 wt% $FeO_{1.5}$–1.2 wt% TiO_2–silica (D). Spectra of both as-prepared samples at 50 °C (upper traces) and samples after dehydration under flowing Ar at 300 °C (lower traces) are shown. Elimination of water leads to a strong reduction in the intensity of the Si–OH band at 980 cm^{-1}. Fe–O–Si species basically remained undetectable. Ti–O–Si moieties give rise to a shoulder in the dehydrated spectra. The ternary Fe-doped titania–silica contains a slightly higher amount of Si–OH groups than the Fe-doped silica and titania–silica.

3.3 Catalytic activity

Fig. 6 gives an overview of possible reactions involved in the liquid-phase oxidation of 2-cyclohexenol by *tert*-butylhydroperoxide (TBHP) in toluene at 90 °C.[14] Reaction (a) leads to the desired epoxide **2** and is mainly catalyzed by Lewis acids, such as titania centers. Reaction (b) is favored by stronger Lewis acids, dehydration of the reactant leads to dimer **3**. Note that this is not an oxidation reaction and does not involve TBHP. The formation of α,β-unsaturated ketone **4** occurs through reaction (c) and probably involves the formation of radical species. The organic peroxide TBHP (**5**) may be decomposed directly and form oxygen and *tert*-butanol [**6**; reaction (d)]. When using pure titania–silica catalysts with less than 3 ppm Fe and less than 1 ppm of all other transition

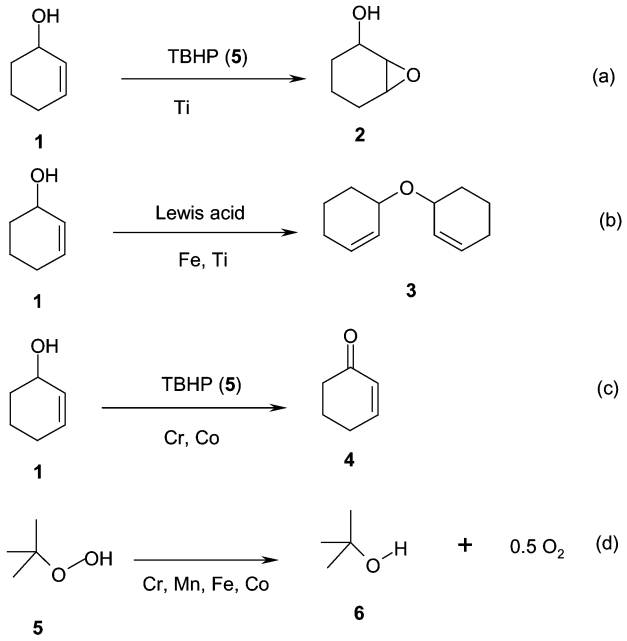

Fig. 6 Chemical reactions involved in the epoxidation of 2-cyclohexenol (**1**) to the corresponding epoxide, **2** [reaction (a)]. Possible side reactions include (b) the formation of dimer **3** due to water abstraction, (c) oxidation to ketone **4**, and (d) the decomposition of TBHP (**5**) to *tert*-butanol (**6**) and oxygen or oxygenated species.

metals, reaction (a) is dominant and good yields (>90%) of the epoxide **2** are obtained. The main side-reaction in the pure titania–silica system is reaction (c), converting about 7% of the reactant to the corresponding ketone.[8] Adding increasing amounts of transition metals changes the activity dramatically. In no reaction, however, were measurable amounts of 2,3-epoxycyclohexanone formed.

Fig. 7 plots peroxide selectivity as a function of dopant concentration for the four transition metals. There is a considerable loss of epoxidation selectivity as the concentrations of all the metals is increased in the titania–silica. Chromium, however, is much more active than the later transition metals as it actually renders the side reaction (c), ketone formation, the dominant process. This is in accord with the fact that Cr is generally known to catalyze the decomposition of hydroperoxides.[29,30] In the case of Mn-doped silica–titania, its stability towards leaching and rather low reactivity are in agreement with the observations of Yonemitsu *et al.*[31] who incorporated Mn in an amorphous SiO_2 matrix by adding Mn ions to MCM-41 and investigated the epoxidation of stilbene by different oxidants. Using TBHP, they found considerable amounts of ketones were formed, while only a fraction of the TBHP decomposed directly. The Mn ions were remarkably stable in the silica matrix and catalyst samples were recycled several times with little loss in activity. The stability of isolated Mn ions in silica correlates with the absence of manganese oxide clusters or crystallites that would result in a signal in the DRUV-VIS spectra. Iron-doped titania–silica exhibits comparatively low hydroperoxide decomposition activity. Spinacé *et al.*[30] investigated Fe-substituted molecular sieves and found they had no activity for the decomposition of cyclohexylhydroperoxide.

Fig. 8 shows the alkene selectivity for the same metal-doped titania–silicas with increasing dopant concentration. While doping with Mn and Fe had little effect on the alkene-related selectivity, Co- and Cr-doped titania–silica consumed considerable amounts of reactant. Leaching experiments showed that significant amounts of Cr entered the reaction mixtures, obviously leading to homogeneous catalysis. For the catalysts containing the other transition metals, leaching was not significant. When reaction mixtures were separated hot from the solids, only marginal differences in activity were found compared to blind mixtures containing the reactants only.

Fe-doped titania–silica contains acidic sites that lead to dimer formation [Fig. 6, reaction (b)]. Beck *et al.*[5] prepared aerogels containing about 2 wt% Fe_2O_3 and observed the formation of large amounts of the same dimer when employing them as catalysts. In our flame synthesis material containing 0.2 wt% Fe_2O_3, however, the dimerization activity is stopped

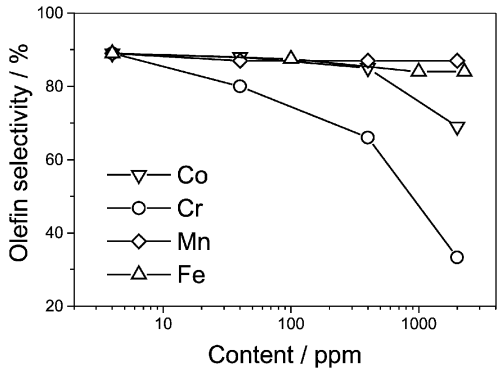

Fig. 8 The selectivity of epoxide formation related to alkene consumption for transition metal-doped titania–silicas. Doping with Cr and Co reduce the efficiency of the alkene usage, while incorporation of Mn and Fe does not lead to significant loss of alkene reactant at dopant levels of up to 2000 ppm. Cr exhibits the most pronounced effect, as it leaches into the reaction mixture, converting most of the substrate to the corresponding ketone.

upon addition of TBHP to the reaction mixture. This new activity correlates with the appearance of a broad peak at 220 to 240 nm in the DRUV-VIS spectrum of the catalyst. To further investigate the nature of this site, a mixture of 2-cyclohexenol and cyclohexanol in the molar ratio of 1 : 3 was added to the 0.2FeTi sample without any TBHP. Fig. 9 shows the corresponding reaction yielding products **8** and **3**. The ratio of **8** (one hydrogenated ring) to **3** (dimer, no hydrogenated ring) is preserved at the initial 1 : 3 ratio. When 0.2FeTi was added to pure cyclohexanol [**7**; reaction (f)], no reaction products were observed. The additional sites on this material are able to produce allyl cations from the 2-cyclohexenol that then react quickly with any nucleophile. This explains why the initial ratio of the two alcohol reactants is preserved in the products in reaction (e). The site is not acidic enough to dehydrate cyclohexanol. After starting the reaction, the weakly basic peroxide probably binds to the Lewis acid site and inhibits the dimerization, while the epoxidation proceeds normally on the Ti sites.

Fig. 10 reports the content of ketone (Fig. 6, compound **4**) in the reaction mixture after 1 h for reference samples (transition metals in pure silica, *i.e.* no titania) and doped titania–silica with 0.2 wt% of the corresponding oxides. No significant differences are found for the two series. Ketone formation is independent of the epoxidation and excludes ternary effects from oxidation reactions involving both Ti and an additional transition metal. The dual Fe–Ti sites in the Fe-containing

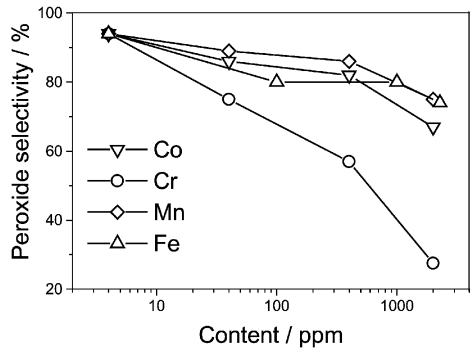

Fig. 7 The selectivity of epoxide formation related to TBHP consumption for transition metal-doped titania–silicas. All metals lead to considerable peroxide decomposition. Cr doping reduced the peroxide selectivity by 20% at only 30 ppm Cr. The high sensitivity of the epoxidation to impurities underlines the importance of clean catalyst preparation.

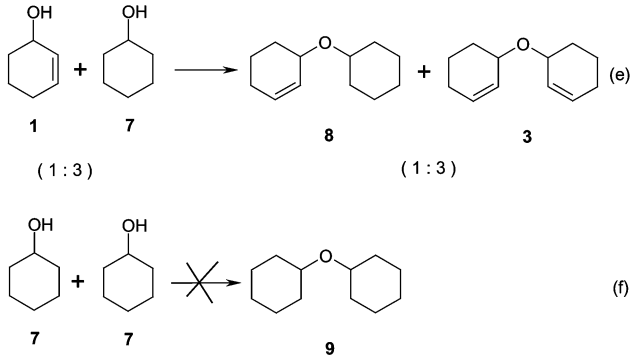

Fig. 9 Chemical reactions used to investigate the acidity of iron sites in flame synthesis titania–silica. The iron sites catalyze the formation of the ethers **8** and **3** in a mixture of 2-cyclohexenol (**1**) and cyclohexanol (**7**), preserving the initial ratio of the alcohol reactants in the products, but are inactive for the dehydration of pure cyclohexanol **7** confirming the formation of an intermediate allyl cation.

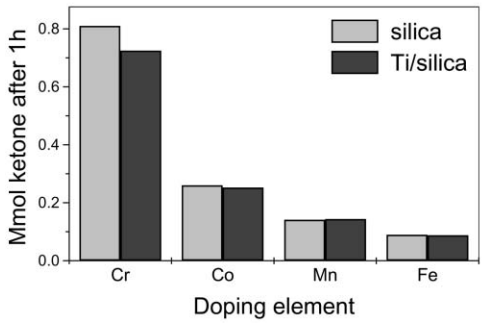

Fig. 10 Amount of by-product ketone **4** formed after 1 h in the reaction mixture for titania–silica and pure silica powders with 0.2 wt% of dopant metals. Oxidation to the ketone is independent of the titania sites and proceeds through radical processes. The difference for chromium-containing materials can be attributed to the high reactivity of Cr, leading to reactant competition between epoxidation and oxidation to the ketone.

materials are not involved in the formation of ketone, only in the non-oxidative dehydration of the 2-cyclohexenol. This agrees well with the fact that the dehydration activity is coupled to the formation of an allyl cation and stopped after addition of TBHP. In the case of chromium, the high reactant conversion led to competition between epoxidation on Ti and oxidation by Cr sites, thereby slightly reducing ketone production in the 0.2CrTi-catalyzed reaction.

4 Conclusions

Catalytic titania–silica nanoparticles with controlled amounts of transition metal dopants (Cr, Mn, Fe, and Co) have been prepared by flame aerosol synthesis. The influence of the dopants on the catalytic behavior of titania–silica in the liquid-phase epoxidation of 2-cyclohexenol strongly depends on the nature of the metal. Metal impurites as low as 40 ppm can dramatically change the epoxidation selectivity of titania–silica-based materials. Chromium is very active in the formation of ketone by-products, while Fe supports the formation of dimers. All investigated metal dopants exhibited some peroxide decomposition activity, leading to reduced peroxide selectivity in titania–silica. These results underline the important role of impurities in titania–silica-based catalysts. Flame synthesis of mixed oxides gives access to particularly pure materials with well-defined compositions, even trace amounts of constituents can be controlled. In a standard experiment, less than 3 ppm transition metals were found in catalysts prepared by flame synthesis. The production of undesirable by-products and process waste may therefore be dramatically reduced.

Acknowledgements

We would like to thank Andreas Hauff and Severin Grewenig for help with the materials synthesis. Financial support granted by the ETH Gesuch Nr 19/01-1 is gratefully acknowledged.

References

1 M. Dusi, T. Mallat and A. Baiker, *Catal. Rev. Sci. Eng.*, 2000, **42**, 213.
2 R. A. Sheldon, M. Wallau, I. Arends and U. Schuchardt, *Acc. Chem. Res.*, 1998, **31**, 485.
3 H. Kochkar and F. Figueras, *J. Catal.*, 1997, **171**, 420.
4 M. Taramasso, G. Perego and B. Notari, *US Pat.*, 4,410,501, 1983 (to Enichem).
5 C. Beck, T. Mallat and A. Baiker, *Catal. Lett.*, 2001, **75**, 131.
6 S. E. Pratsinis and S. V. R. Mastrangelo, *Chem. Eng. Prog.*, 1989, **85**, 62.
7 S. E. Pratsinis, *Prog. Energy Combust. Sci.*, 1998, **24**, 197.
8 W. J. Stark, S. E. Pratsinis and A. Baiker, *J. Catal.*, 2001, **203**, 516.
9 W. J. Stark, K. Wegner, S. E. Pratsinis and A. Baiker, *J. Catal.*, 2001, **197**, 182.
10 S. E. Pratsinis, W. H. Zhu and S. Vemury, *Powder Technol.*, 1996, **86**, 87.
11 H. Briesen, A. Fuhrmann and S. E. Pratsinis, *Chem. Eng. Sci.*, 1998, **53**, 4105.
12 D. Günther, R. Frischknecht, C. A. Heinrich and H.-J. Kahlert, *J. Anal. At. Spectrom.*, 1997, **12**, 939.
13 D. Günther and C. A. Heinrich, *J. Anal. At. Spectrom.*, 1999, **15**, 1363.
14 C. Beck, T. Mallat, T. Bürgi and A. Baiker, *J. Catal.*, 2001, **204**, 428.
15 H. E. B. Lempers and R. A. Sheldon, *Stud. Surf. Sci. Catal.*, 1997, **105**, 1061.
16 J.-D. Grunwaldt, C. Beck, W. J. Stark, A. Hagen and A. Baiker, *Phys. Chem. Chem. Phys.*, 2002, **4**, 3514.
17 P. Wu, T. Tatsumi, T. Komatsu and T. Yashima, *Chem. Lett.*, 2000, **7**, 774.
18 A. Carati, C. Flego, E. Previde Masara, R. Millini, L. Carluccio and G. Bellussi, *Microporous Mesoporous Mater.*, 1999, **30**, 137.
19 S. Bordiga, F. Geobaldo, C. Lamberti, A. Zecchina, F. Boscherini, F. Genoni, G. Leofranti, G. Petrini, M. Padovan, S. Geremia and G. Vlaic, *Nucl. Instrum. Methods Phys. Res., Sect. B*, 1995, **97**, 23.
20 S. Bordiga, R. Buzzoni, F. Geobaldo, C. Lamberti, E. Giamello, A. Zecchina, G. Leofranti, G. Petrini, G. Tozzola and G. Vlaic, *J. Catal.*, 1995, **158**, 486.
21 G. Centi and F. Vazzana, *Catal. Today*, 1999, **53**, 683.
22 A. Tuel, I. Arcon and J. M. M. Millet, *J. Chem. Soc., Faraday Trans.*, 1998, **94**, 3501.
23 S. J. Ma, L. S. Li, F. P. Sun and S. L. Qiu, *Chem. J. Chin. Univ.*, 1997, **18**, 504.
24 R. L. White and A. Nair, *Appl. Spectrosc.*, 1990, **44**, 69.
25 M. Schraml-Marth, K. L. Walther, A. Wokaun, B. E. Handy and A. Baiker, *J. Non-Cryst. Solids*, 1992, **143**, 93.
26 E. F. Vansant, P. Van Der Voort and K. C. Vrancken, *Stud. Surf. Sci. Catal.*, 1995, **93**, 3.
27 N. Maxim, A. Overweg, J. Kooyman, J. H. M. C. van Wolput, R. W. J. M. Hanssen, R. A. van Santen and C. L. Abbenhuis, *J. Phys. Chem. B*, 2002, **106**, 2203.
28 D. C. M. Dutoit, M. Schneider and A. Baiker, *J. Catal.*, 1995, **153**, 165.
29 Z. Muzart, *Chem. Rev.*, 1992, **92**, 13.
30 E. V. Spinacé, U. Schuchardt and D. Cardoso, *Appl. Catal. A*, 1999, **185**, 193.
31 M. Yonemitsu, Y. Tanaka and M. Iwamoto, *J. Catal.*, 1998, **178**, 207.